ANL-6738

Argonne National Laboratory

DEVELOPMENT OF AN ELECTRICAL RESISTIVITY PROBE FOR VOID-FRACTION MEASUREMENTS IN AIR-WATER FLOW

by

George P. Nassos

ANL-6738
Engineering and Equipment
(TID-4500, 22nd Ed.)
AEC Research and
Development Report

ARGONNE NATIONAL LABORATORY
9700 South Cass Avenue
Argonne, Illinois 60440

DEVELOPMENT OF AN ELECTRICAL RESISTIVITY PROBE FOR VOID-FRACTION MEASUREMENTS IN AIR-WATER FLOW

by

George P. Nassos
Northwestern University

Reactor Engineering Division, ANL
and
Associated Midwest Universities

This report is one of a series that describes heat transfer and fluid-flow studies performed at Argonne under a program sponsored jointly by the Associated Midwest Universities and the Argonne National Laboratory.

The earlier reports in this series are ANL-6625, ANL-6667, ANL-6674, and ANL-6710.

This report has been reproduced from a thesis submitted in Partial Fulfillment of the Requirements for the Degree of Master of Science in Chemical Engineering in the Graduate School of Northwestern University.

June 1963

Operated by The University of Chicago
under
Contract W-31-109-eng-38
with the
U. S. Atomic Energy Commission

TABLE OF CONTENTS

LIST OF FIGURES

LIST OF TABLES

DEVELOPMENT OF AN ELECTRICAL RESISTIVITY PROBE FOR VOID-FRACTION MEASUREMENTS IN AIR-WATER FLOW

by

George P. Nassos

ABSTRACT

Work has been done on the adaptation of an electrical probe, developed by Neal[9] for the measurement of local void fractions in mercury-nitrogen flow, to air-water flow. The adaptation is more difficult because of wetting of the probe by water. Various probe shapes and filming agents were employed without great success. Some improvement was obtained by means of a separate triggering circuit, but the calculated void fraction was still somewhat low compared with that measured by the gamma-ray-attenuation technique. Presumably, this is due to a finite response time of the probe, associated with the wetting of the tip; hence, further development of this technique is necessary.

I. INTRODUCTION

Two-phase flow is used to describe the simultaneous flow of a liquid and gaseous phase, either cocurrently or countercurrently. The distribution of the two phases depends mainly on the volumetric flow rate of each phase. Various flow regimes can be distinguished, depending upon the Reynolds, Froude, and Weber numbers, as well as upon β, the volumetric flow concentration. For low values of β in vertical pipes, the gas tends to be distributed as a suspension of small bubbles (bubble-flow regime). As β increases, small bubbles tend to coalesce, forming larger bubbles which almost fill the channel cross section. This regime is called slug flow. Upon further increase in the gas flow rate, the slug length increases until the core of the pipe is filled with gas and the liquid flows along the wall as an annular film (annular-flow regime). At still higher gas velocities, the liquid tends to be dispersed into the gas phase as a mist (mist-flow regime).

Although there is interest in all four flow regimes, bubble and slug flows are observed in most cases of practical importance. In the study of these two basic flow patterns, some of the parameters of interest are void

fraction, bubble-size distribution, and bubble frequency. An electrical resistivity probe was introduced by Neal[9] for the measurement of these parameters in cocurrent mercury-nitrogen flow. This probe, however, could not be used directly for measurements in air-water flow because of increased wetting of the probe tip.

This report describes work in the development of an electrical resistivity probe for measurements of the local void fraction in air-water flow in which the liquid can be considered to be a continuous phase. In addition to permitting this useful measurement, it is hoped that the probe will provide information with which to compare the two-phase flow models proposed, among others, by Bankoff[1] and Levy[8].

II. REVIEW OF LITERATURE

Because of its great importance in two-phase flow and studies of boiling phenomena, techniques for the measurement of void fraction have been given considerable attention. A literature survey of these techniques was conducted by Gouse,[4] who summarized the results in tabular form. A few methods of void-fraction measurement are reviewed in the following discussion.

Johnson and Abou-Sabe[7] placed special disk-type valves, of uniform tube diameter when open, at each end of the test section. The spring-loaded valves were closed rapidly and simultaneously so as to isolate the contents of the test section.

Zuber and Hench[14] modified the pressure-drop technique by fixing one tap near the bottom of the test section and placing a movable tap near the top. The manometer leg connected to the fixed tap was filled with water, and the other leg was filled with air by bleeding a small amount of air into this leg so that it bubbled out of the upper tap very slowly. By observing the manometer readings before and after the air flow was initiated, the average void fraction between the two taps was determined.

Dengler[2] used a tracer technique to determine voids. A radioactive salt, $Mn^{52}Cl_2$, was dissolved in the liquid phase. If the salt did not coat the interior walls, the count was proportional to the liquid fraction.

The gamma-ray-attenuation method was studied by Hooker and Popper.[6] This technique employs a radioactive source and a crystal detector. The strength of the attenuated beam passing through the stream is a function of the stream density and, therefore, related to the void fraction. Petrick[11] improved this method by traversing the source and detector across the channel width, and thus obtained a density profile. Petrick[10] also introduced a polynomial-fitting technique for determining local void fractions in a round pipe. Beta rays have also been used in place of gamma rays.[13]

Neal[9] constructed an electrical probe for measuring local parameters in mercury-nitrogen flow. The probe consists of an insulated needle with an exposed tip pointing into the flow. When a battery and a resistor in series with the probe was connected to ground, a change in voltage was observed as mercury and then nitrogen came into contact with the probe. This electrical probe was developed in a system where the continuous phase was a liquid metal. The purpose of the present work, therefore, was to extend this technique to air-water flow.

After the present work was essentially completed, the author learned* that a probe similar to the one developed by Neal had been independently constructed by Solomon[12] for use as a flow-regime indicator in two-phase air-water flow. Solomon's principal interest was in detecting changes in flow configuration, whereas the present work was aimed at determining local void fractions and bubble-size distributions.

*Private communication from Dr. P. Griffith to Dr. S. G. Bankoff

III. EXPERIMENTAL APPARATUS

A. Flow System

The arrangement of the flow system used in these studies is shown pictorially in Figure 3.1 and schematically in Figure 3.2. This natural-circulation loop consists of a water- and air-injection system, the test section, and an air-water separator. The metered streams of air and water were fed to the bottom of the test section. The resulting two-phase mixture flowed up through the test section and into the separator where the air was liberated to the atmosphere and the water was returned to the test section via a downcomer by gravity. The flow system was constructed almost entirely of Lucite to allow for visual observation.

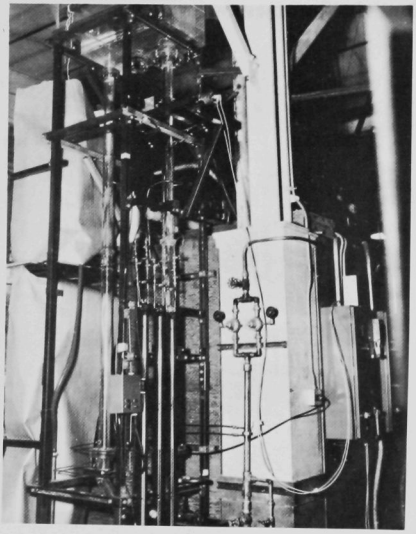

112-2733

Fig. 3.1. Experimental Apparatus

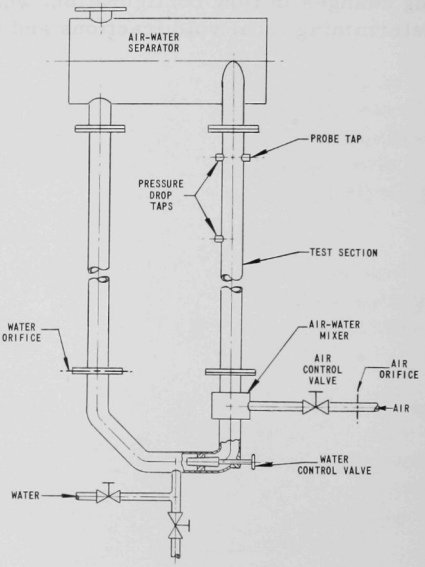

Fig. 3.2. Schematic Diagram of Flow System

1. Description of Equipment Components

A cross-sectional view of the water- and air-injection system is shown in Figure 3.3. The air entered through two 1-in. copper tubes and merged with the vertically flowing water stream through 168 holes spaced along the periphery of the pipe.

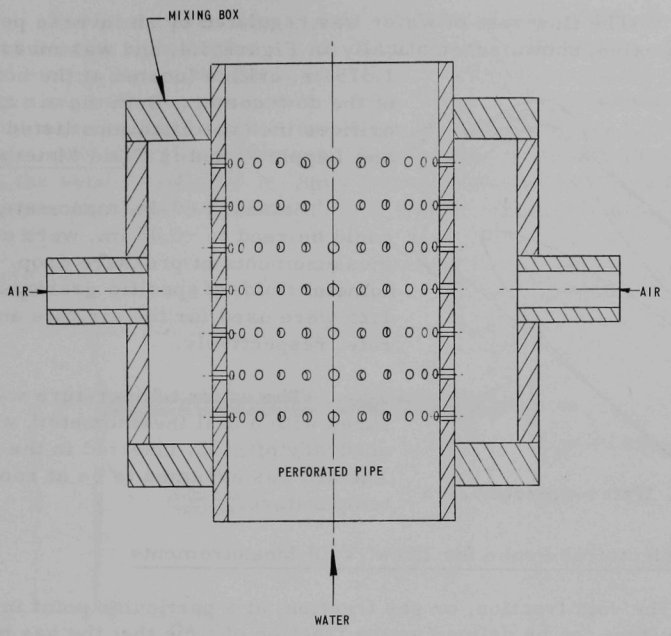

Fig. 3.3. Sectional View of Air-Water Mixer

The test section was constructed from an $8\frac{1}{2}$-ft piece of $2\frac{3}{4}$-in. Lucite pipe. Six probe taps, spaced equally 1 ft apart, were inserted to allow for probe measurements to be made at various distances from the air injector.

The separator was a 33 x 24 x 18-in. Lucite tank with an opening in the top. The velocity of the two-phase mixture entering the separator decreased sufficiently, due to the increase in cross-sectional area, allowing the air to be completely removed from the water. The water then entered the $2\frac{3}{4}$-in. downcomer.

The air supply was obtained from the main laboratory line, and the water supply was obtained from the main tap-water line. Tap, rather than demineralized, water was used because of its higher electrical conductivity, a necessity for proper functioning of the probe.

2. Instrumentation and Control

The flow rate of air was regulated by two needle valves and measured at a 0.125-in. orifice. A constant pressure of 70 psig was maintained upstream from the orifice by two Norgen regulators.

The flow rate of water was regulated by an inverse percentage-flow plug valve, shown schematically in Figure 3.4, and was measured at a 1.375-in. orifice located at the bottom end of the downcomer. Both the air and water orifices met specifications listed in Grace and Lapple[5] and in Fluid Meters.[3]

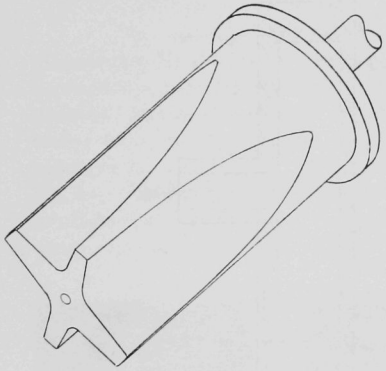

Fig. 3.4. Water-control Valve

Standard 60-in. manometers, which could be read to ±0.05 in., were used for measurements of pressure drop. Manometer fluids of specific gravity 2.95 and 1.25 were used for the air rate and water rate, respectively.

The water temperature was measured with a dial thermometer, with an accuracy of ±1°C, inserted in the separator. The air was assumed to be at room temperature.

B. An Electrical Probe for Local Void Measurements

The void fraction, or gas fraction, at a particular point in a two-phase system can be defined as the fraction of time that the gas phase exists at the point in question. This can be stated mathematically as follows:

$$\alpha = \frac{1}{T}\int_0^T [1-f(t)]\,dt \quad , \tag{3.1}$$

where α is the void fraction, f(t) is a discontinuous function of time that assumes a value of one when the liquid phase exists at the point in question and a value of zero when the gas phase exists at the point, and T is the time interval over which the void fraction is determined. The interval T must be large enough that a statistically good average can be obtained at that point.

1. The Probe

An electrical probe, capable of measuring instantaneously the local resistivity of a two-phase mixture, and thereby providing a measure of local values of void fraction, was developed. When air is in contact with the probe tip, the resistance between the probe and ground is infinite, whereas when water is in contact with the probe, the resistance is about 75,000 ohms. By connecting a battery and a resistor in series with the probe, the voltage drop across the resistor could be observed.

The probe (see Figure 3.5) consists of a 6-in. length of 0.031-in. steel wire bent at right angles $1\frac{1}{4}$ in. from one end. By means of an oil stone and emery paper, the tip of the shorter segment was filed to a point. The longer segment was encased in a 4-in. piece of $\frac{1}{8}$-in. stainless steel tubing, but was insulated from it by Teflon "spaghetti." The filed piece was insulated by a Krylon spray enamel. In order to assure complete insulation, the bend was dipped in liquid paraffin and allowed to cool. The probe tip was then carefully scratched to expose about 0.01 in. of the point.

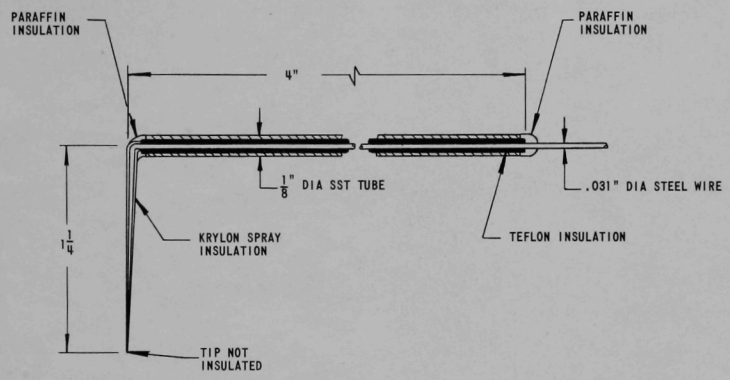

Fig. 3.5. Electrical Probe

Upon completion of the probe, it was inserted in the channel by means of a modified "Swagelock" tube fitting. The first ferrule of the fittings was replaced by a $\frac{1}{8}$-in. O-ring, and the second ferrule was reversed. This allowed the probe to be traversed across the pipe and at the same time remain leak proof. The probe was oriented with the exposed tip pointing into the direction of flow (see Figure 3.6).

2. The Integrating Circuit

In order to determine what fraction of time gas was in contact with the probe tip, the probe signal was electronically integrated for a time T. The integrating circuit is shown schematically in Figure 3.7 and, along with the other electrical components, pictorially in Figure 3.8. It can easily be shown that this circuit yields the following relationship:

$$e_0 = -\frac{1}{RC}\int_0^T e(t)\,dt \quad . \tag{3.2}$$

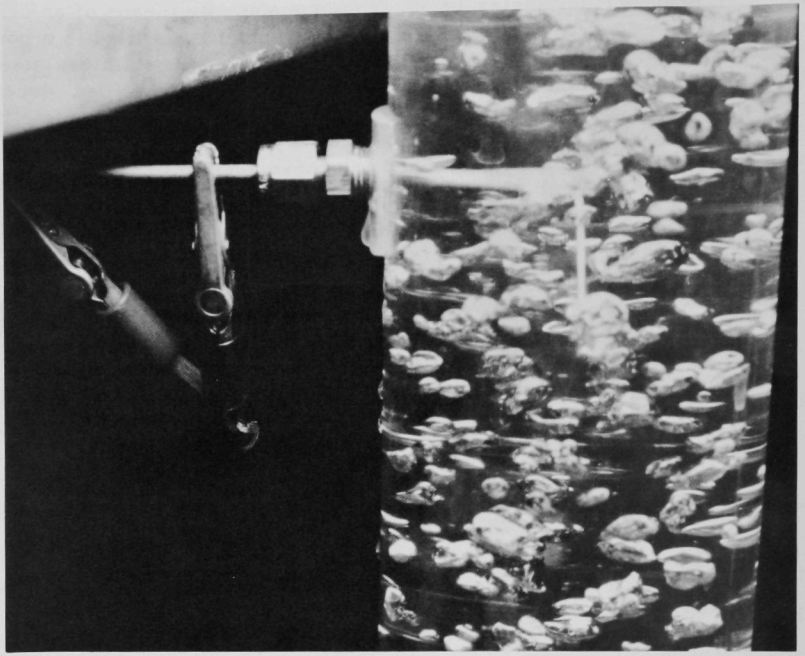

112-2735

Fig. 3.6. Probe in Channel

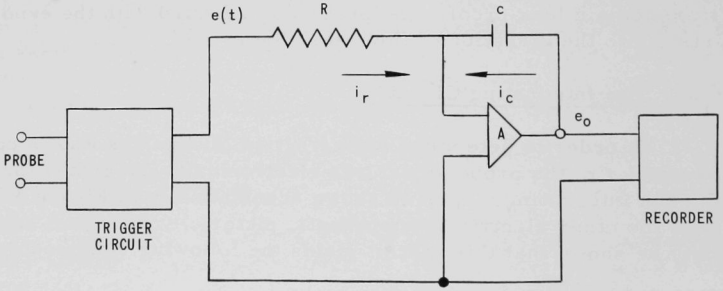

Fig. 3.7. Integrating Circuit

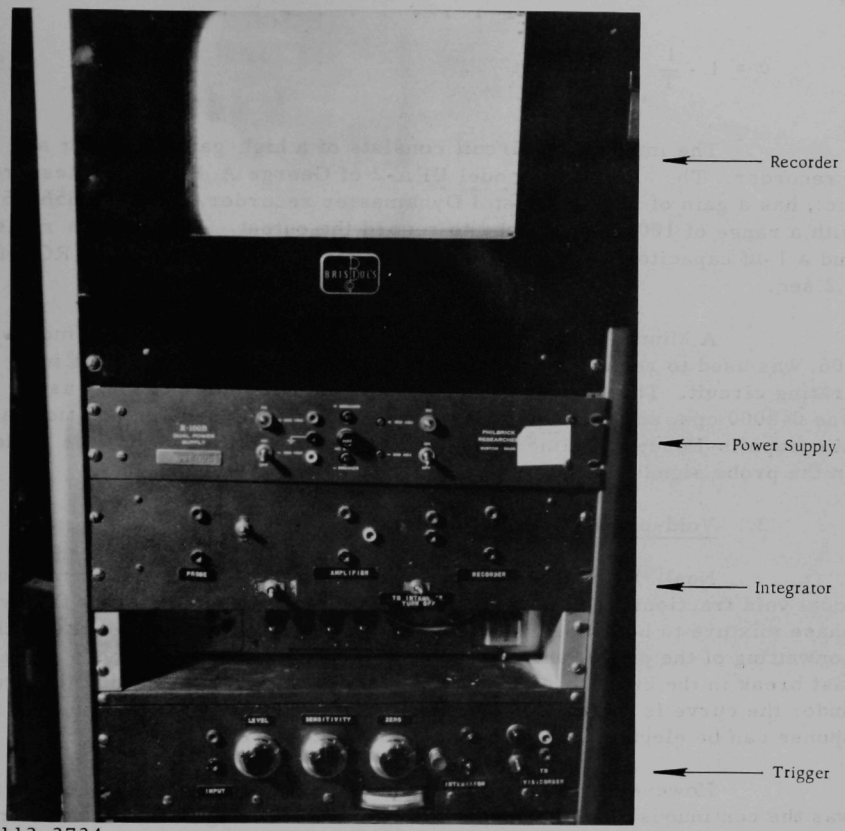

Fig. 3.8. Electrical Equipment

Upon multiplying this equation by the constant - RC/ET, one obtains:

$$-e_0 \frac{RC}{ET} = \frac{1}{T} \int_0^T \frac{e(t)}{E} dt \quad . \tag{3.3}$$

By comparing equations (3.1) and (3.3) and noticing that e(t)/E and f(t) have identical properties, one can then write:

$$1 - \alpha = \frac{1}{T} \int_0^T \frac{e(t)}{E} dt \tag{3.4}$$

or

$$\alpha = 1 - \frac{1}{T} \int_0^T \frac{e(t)}{E} \, dt \quad . \tag{3.5}$$

The integrating circuit consists of a high-gain amplifier and a recorder. The amplifier, model UPA-2 of George A. Philbrick Researches, Inc., has a gain of 10^7. A Bristol Dynamaster recorder, model IPH560-51, with a range of 100 mv was used to record the output. A 2.2-Mohm resistor and a 1-μf capacitor were used to give the circuit a time constant (RC) of 2.2 sec.

A Minneapolis-Honeywell eight-channel "Visicorder," model 906, was used to record the probe signal which was the input to the integrating circuit. The frequency response of the particular channel used was 0-2000 cps, and the paper drive was set at 25 in./sec. In addition, a Minneapolis-Honeywell timer was used in order to introduce a time scale on the probe signal record.

3. Void-probe Trigger

Neal(9) stated that, when using a probe of this type for measuring local void fractions, it is advantageous for the continuous phase of the two-phase mixture to be a liquid metal. The high surface energy results in the nonwetting of the probe, and a fast break in the circuit is obtained. With a fast break in the circuit, a square-wave response is obtained, and the area under the curve is directly proportional to the liquid fraction. Thus the response can be electronically integrated as stated previously.

However, in the system under study, water, which wet the probe, was the continuous phase, and this meant that the change in resistance from 75,000 ohms to infinity was gradual and not sharp enough to obtain square waves. Therefore, in order to apply electronic integration, the probe signal response had to be altered to a square-wave response such that the fraction of the total time that liquid was in contact with the probe was the same for both response curves.

The problem was solved by employing an electronic circuit designed by T. T. Anderson. This circuit, shown in Figure 3.9, consists of two principal components: a transistorized electrometer amplifier, and a transistorized Schmitt trigger circuit.

The Schmitt trigger circuit contains three potentiometers, the sensitivity, level, and zero "pots." The sensitivity and level potentiometers, which are located at the input, are adjusted either to fire or turn off the trigger when the amplifier output voltage begins to drop from a level corresponding to air in contact with the probe tip. The trigger will then turn

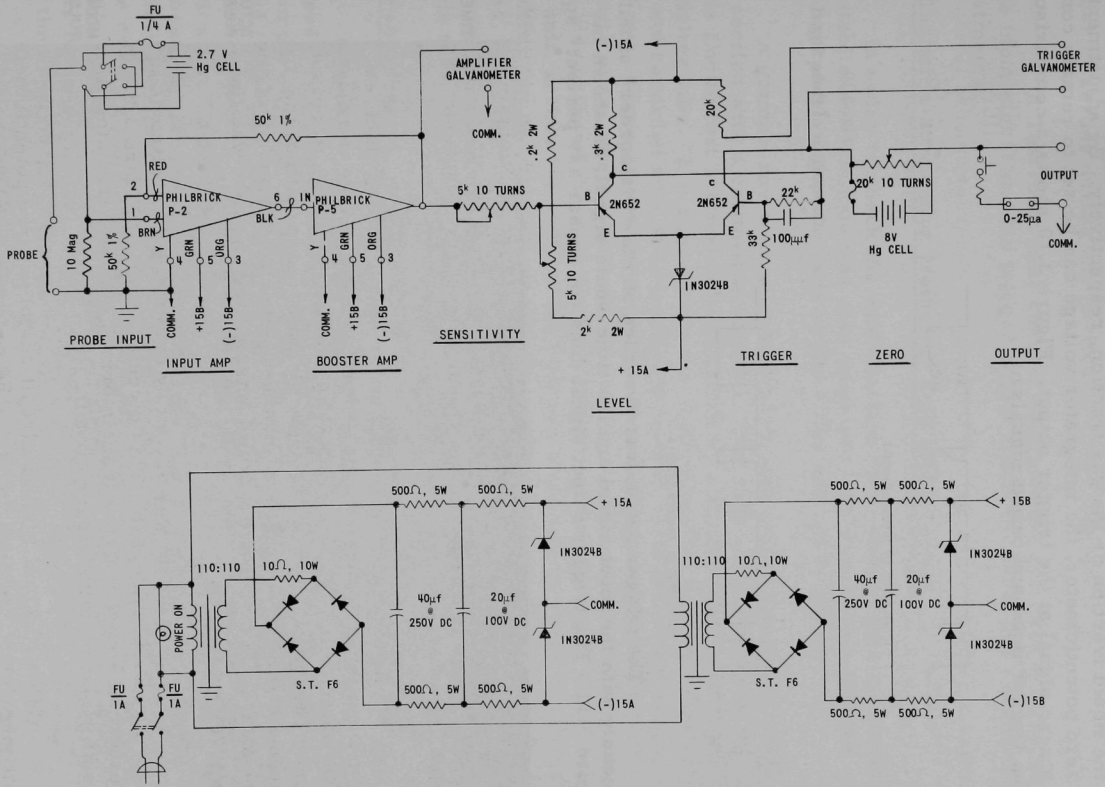

Fig. 3.9. Void-probe Trigger

off or fire when the amplifier output returns to the original voltage level. The trigger can be biased on or off by making the input voltage either negative or positive. This corresponds to integrating electronically either for the liquid fraction or the gas fraction, respectively. By adjustment of the zero potentiometer, the integrator voltage can be set to remain constant for a zero signal at the trigger output. Figure 3.10 shows a comparison of the trigger input and output signals.

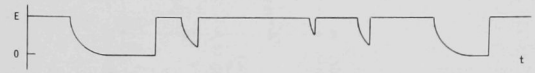

(a) INPUT TO TRIGGER CIRCUIT

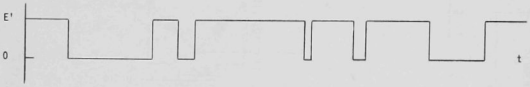

(b) OUTPUT OF TRIGGER CIRCUIT

Fig. 3.10
Comparison of Probe Signal

The trigger output was recorded on the "Visicorder" simultaneously with the input signal and the time-scale signal, as shown in Figure 3.11. The trigger output signal does not appear as "perfect" square

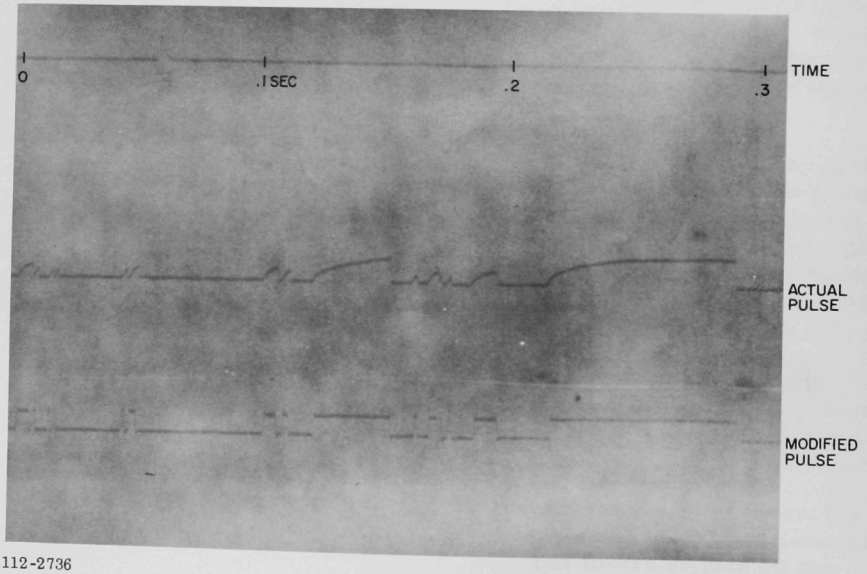

112-2736

Fig. 3.11. Probe Signals

waves because the frequency response of the particular galvanometer used in the "Visicorder" was only 0-600 cps, although the integrating circuit input was a pseudo-random square wave, i.e., a square wave with a random number of zeroes during any particular time interval.

A Tektronix dual-channel oscilloscope was used to observe the probe input signal and the trigger output signal for level and sensitivity adjustments.

C. Radiation-attenuation Method of Void Measurement

In order to check the void-fraction data obtained with the probe, an established technique was also employed. This technique depends on the absorption of gamma rays by the water and not by the air.

A gamma-ray source, thulium-170, was placed about 4 in. from the test section with a collimator between. The rays not absorbed by the water or the Lucite test section were collected by a scintillation crystal photomultiplier tube. The signal from the photomultiplier tube was then amplified and recorded on a Minneapolis-Honeywell recorder with a range of 0-10 mv. Since gamma rays are not absorbed appreciably by air, the strength of the attenuated beam is a function of the stream density and, thus, a function of the void fraction. By traversing the source and collector, as a unit, across the width of the channel, a continuous curve of chordal densities can be obtained, whence the average void fraction can be determined. This technique requires traversing an empty channel, a full channel, and the two-phase mixture. The theory and derivation of equations of this technique were shown by Petrick.(11)

D. Procedure

Before the flow system was filled with water, the test section was traversed horizontally with the gamma-ray equipment to obtain a trace of the empty channel. At the same time, the integrator recorder was allowed to run for 60 sec. This output signal corresponds to a value of $\alpha = 1.0$. From equation (3.2), this signal is simply - ET/RC and is the quantity by which all succeeding output signals were divided to obtain the gas fraction. By means of this technique the exact value of the integration time constant RC need not be known. However, each succeeding integration should be made over the same interval, T = 60 sec, and the quantity ET/RC should remain constant for the entire experiment. Since the value ET/RC is a linear function of time, a different integration interval can be used, but then the constant ET/RC must be changed accordingly.

It should be noted that a positive input voltage was applied on the trigger, biasing the input transistor "off" and thus integrating directly for

the quantity α. Therefore, equation (3.4) should be rewritten as

$$\alpha = \frac{1}{T} \int_0^T \frac{e(t)}{E} \, dt \quad . \tag{3.6}$$

After filling with water, the test section was traversed to obtain a full-channel trace. Air was then bubbled through the test section, the air and water valves being adjusted for the proper flow rates. Again the test section was traversed with the gamma-ray equipment to obtain the two-phase trace.

The level and sensitivity adjustments were made by observing the trigger input and output signals on the oscilloscope. The zero adjustment was made by "zeroing" the Simpson meter provided for this purpose. With the flow rates constant, the complete void-fraction profile was obtained by integrating the probe signal at each of seven radial positions and using equation (3.6) and the constant - ET/RC.

A photographic record of the probe signal, shown in Figure 3.11, was obtained by allowing the "Visicorder" to run for 15 sec, which corresponds to a 30-ft trace of signal.

IV. DISCUSSION AND RESULTS

A. Probe Wetting

The program for development of the probe commenced with preliminary experiments conducted in a 4-gal jar. The originally designed probe was suspended in the water-filled jar, and air was slowly bubbled up through a 1-in. Lucite cylinder toward the probe. A 1.5-v battery and 100,000-ohm resistor were connected in series with the probe to ground, and the voltage drop across the resistor was observed on an oscilloscope. The pulse signal revealed that a sharp break in the circuit did not occur when the bubble was pierced by the probe; instead, the change in voltage drop assumed an exponential path when going from a voltage corresponding to water surrounding the probe tip to zero, which corresponds to air surrounding the probe tip.

The cause of this irregularly shaped response was believed to be the water adhering to the probe when air was actually surrounding it. The probe was, therefore, insulated with Teflon, and the tip was then carefully scratched so as to expose the steel point. This, however, did not solve the problem, probably because the exposed tip was wetted even though the remaining part of the probe was not. Figure 4.1 shows what is believed to be actually happening as an air bubble approaches the probe tip. In position 1 the bubble is approaching the probe, whereas in position 2 the probe is just touching the bubble surface. Since the probe is still in the liquid medium, the circuit is closed and a voltage drop across the resistor equal to E appears on the oscilloscope. The probe then begins to pierce the bubble (position 3), but a small quantity of water (exaggerated in the figure to clarify the theory) remains on the probe tip, causing the voltage gradually to decay from a value of E to zero. When the probe is completely surrounded by air (position 4) an open circuit is created until the probe again reaches the air-liquid interface (position 5), thus creating a closed circuit and sending the voltage to the original value of E.

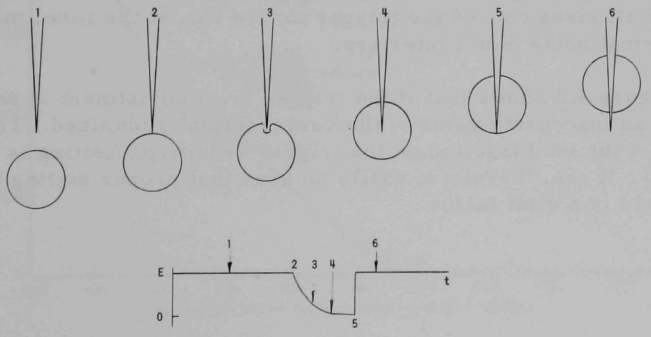

Fig. 4.1. Probe Wetting

The distance traversed by the probe into the bubble before the tip was completely surrounded by air could be determined by recording the pulse on the "Visicorder" and visually estimating the bubble velocity. From the assumption that the bubble velocity is 2 ft/sec and a measurement of the "wetted" distance as $\frac{1}{2}$ in. on a time scale of 25 in./sec, it may be calculated that the probe penetrates a distance of about $\frac{2}{3}$ in. into the bubble. Although bubbles smaller than $\frac{2}{3}$ in. will be detected by the probe, only those larger than this value will cause the observed voltage to drop to a zero value.

Since integrating the signal depends on a square-wave pulse, the trigger circuit described in the previous chapter was introduced in the integrating circuit. A slight deviation from E of the probe signal voltage would cause the trigger to "turn off," and the trigger output voltage would drop instantly from a value of E' to zero. Upon returning to the original value of E, the probe signal voltage would cause the trigger to "fire," and then the trigger output voltage would instantly return to its original value of E', as shown in Figure 3.10. Integrating the trigger output signal would result in obtaining the liquid fraction $1 - \alpha$. However, reversal of the polarity of the trigger input would cause the trigger to "fire" when the probe pierces the bubble and "turn off" when it is again surrounded by liquid; integration of this signal gives the gas fraction α. This procedure was utilized for all the experimental data.

By adjusting the "level" potentiometer, the voltage value of the probe signal at which the trigger would "fire" could be set at any desired level. Adjusting the "sensitivity" potentiometer would minimize the difference between the voltage levels for "firing" and "turning off." If the trigger voltage level is set too close to the probe voltage E, noise in the electrical circuit could cause the trigger to "fire" even when no bubble is present. On the other hand, if the trigger level is not set close enough, small bubbles could pierce the probe without "firing" the trigger. The optimum setting of the two adjustments was made by observing the probe and trigger output signals on a dual-channel oscilloscope and noticing when bubbles of all sizes caused the trigger to fire but, at the time, making sure that electrical noise didn't interfere.

Figure 4.2 shows that if the trigger level adjustment is not set properly, an inaccurate value of the void fraction is obtained. The dependence of the void fraction on the trigger sensitivity setting is shown in Figure 4.3. It can, therefore, easily be seen that proper setting of these two controls is a vital factor.

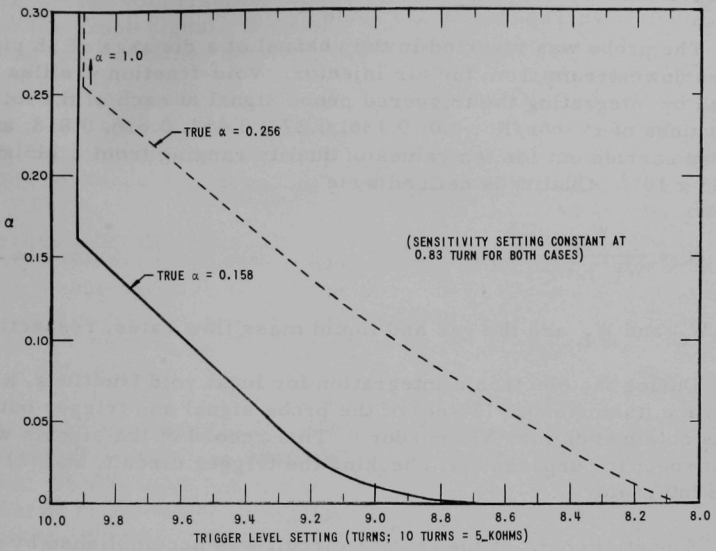

Fig. 4.2. Dependence of Void Fraction on Trigger Level Setting

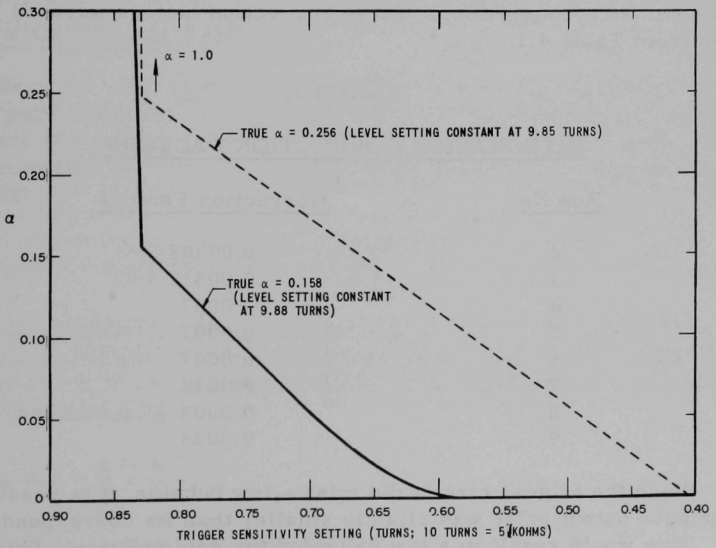

Fig. 4.3. Dependence of Void Fraction on Trigger Sensitivity Setting

B. Integration of Probe Signal

The probe was inserted in the channel at a distance of 35 pipe diameters downstream from the air injector. Void-fraction profiles were obtained by integrating the triggered probe signal at each of the following seven values of $r' = r/R$: 0.0, 0.136, 0.273, 0.454, 0.636, 0.818, and 1.00. This was carried out for ten values of quality ranging from 1.145×10^{-4} to 1.045×10^{-3}. Quality is defined by

$$X = \frac{W_G}{W_L + W_G} \quad , \tag{4.1}$$

where W_G and W_L are the gas and liquid mass flow rates, respectively.

During the electronic integration for local void fractions, a 30-ft trace (taking about 15 sec) of the probe signal and trigger output signal was obtained on the "Visicorder." This record of the signals was used for two specific purposes: (1) checking the trigger circuit, and (2) checking the integrator.

A partial check of the trigger circuit was accomplished by simply looking for all the bubble pulses that did not "fire" the trigger. The total dwell time of these "missed" bubbles was obtained by summing the dwell times of the individual bubbles. Division by the total time elapsed (15 sec) resulted in a number corresponding to a void fraction to be added to those values obtained by integration. These correction factors were all small, as seen from Table 4.1.

Table 4.1

INTEGRATION CORRECTION FACTORS

Run No.	Correction Factors
2	0.00308
3	0.00317
4	0.0007
5	0.0007
6	0.0007
7	0.0012
8	0.0003
9	0.0025

Since the trigger circuit did miss a few bubbles, it is possible that each trigger output pulse was slightly smaller than its corresponding probe pulse. This would result in a low value for the void fraction. This error, along with any error in the electronic integration, was checked as follows.

One value for the void fraction was obtained manually from the photographic record of the probe signal. A comparison between this value and its corresponding value obtained from the integrator shows a small error, as seen in Table 4.2.

Table 4.2

CHECK OF INTEGRATION

α (manually determined)	α (electronically determined)
0.3004	0.290
0.2232	0.224
0.1237	0.126

In each experimental run, the photographic record of the trigger input and output signals was obtained by allowing the "Visicorder" to run for 15 sec. Preliminary calculations had been made to determine whether an interval of 15 sec would give a statistically good average value for the void fraction. A trace corresponding to 20 sec was used to calculate manually the void fraction for each of four 5-sec intervals and also for the first 10 sec, 15 sec, and 17 sec, as well as for the entire trace. Each value obtained came within 10% of the total average value, while that value for the first 15 sec came within 1%.

C. Use of Gamma-ray Technique

Since the electrical probe technique is the first capable of measuring local or point values of void fraction, there are no previous data with which to compare the results. However, the void-fraction profile can be checked by assuming that the void fraction can be expressed as a function of the polynomial

$$\alpha_r = \sigma + a\left(\frac{r}{R}\right)^2 + b\left(\frac{r}{R}\right)^4 + c\left(\frac{r}{R}\right)^6 \quad , \tag{4.2}$$

which is an equation in four unknowns: σ, a, b, and c. By means of the gamma-ray technique, chordal densities can be found at four radial positions, say r = 0, 0.4 R, 0.6 R, and 0.8 R. The problem then reduces to solving simultaneously

$$\bar{\alpha}_0 = \sigma + \frac{a}{3} + \frac{b}{5} + \frac{c}{7} \tag{4.3}$$

$$\bar{\alpha}_{0.4R} = \sigma + 0.44a + 0.256b + 0.1779c \tag{4.4}$$

$$\bar{\alpha}_{0.6R} = \sigma + 0.573a + 0.365b + 0.255c \tag{4.5}$$

$$\bar{\alpha}_{0.8R} = \sigma + 0.76a + 0.587b + 0.465c \tag{4.6}$$

for the four unknowns. Derivation of these equations is shown in reference (10).

In addition to the void-fraction profile, the cross-sectional average value was checked. This value was obtained by graphical integration of the profile determined by the probe method, and from the gamma-ray technique by substituting equation (4.2) into

$$\bar{\alpha} = \frac{\int_0^R 2\pi r \alpha_r dr}{\int_0^R 2\pi r dr} \quad . \tag{4.7}$$

The latter value was also compared with the average value obtained from a complete traverse of the channel. This was done in order to validate, to some degree, the polynomial fit.

D. Comparison of the Two Techniques

The void-fraction data obtained by the probe method are plotted along with the polynomial profiles, given as solid lines, in Figures 4.4-4.13.

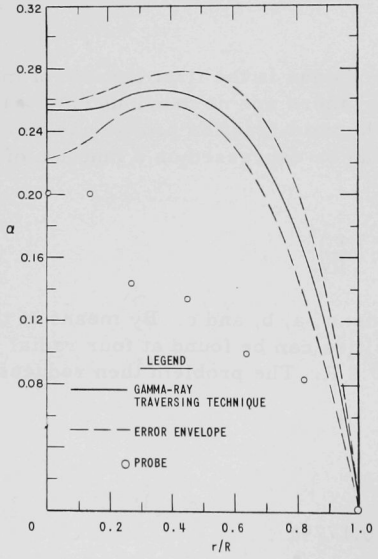

Fig. 4.4

Void Profile for
$X = 5.35 \times 10^{-4}$

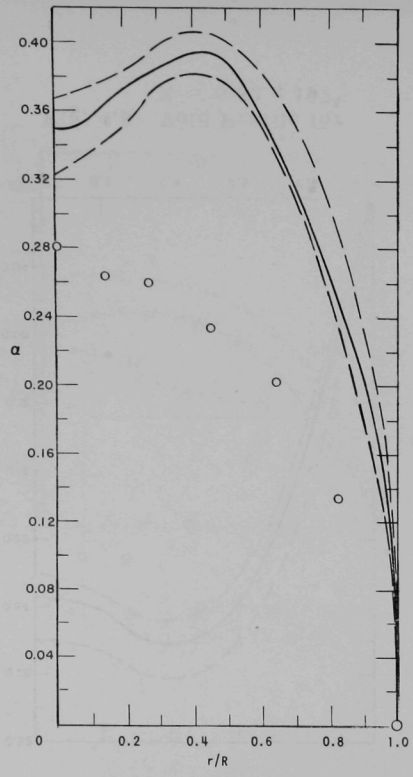

Fig. 4.5. Void Profile for $X = 8.15 \times 10^{-4}$

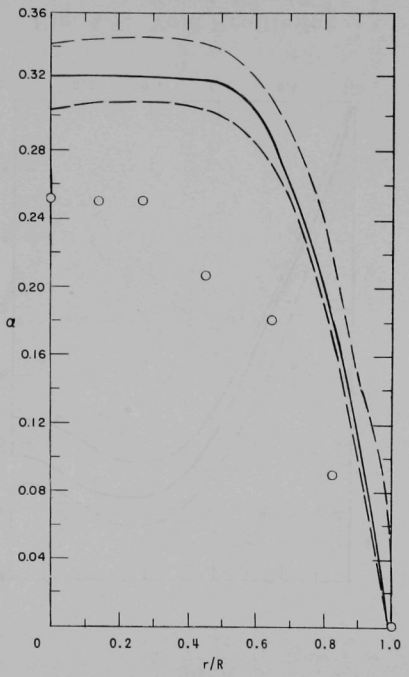

Fig. 4.6. Void Profile for $X = 6.48 \times 10^{-4}$

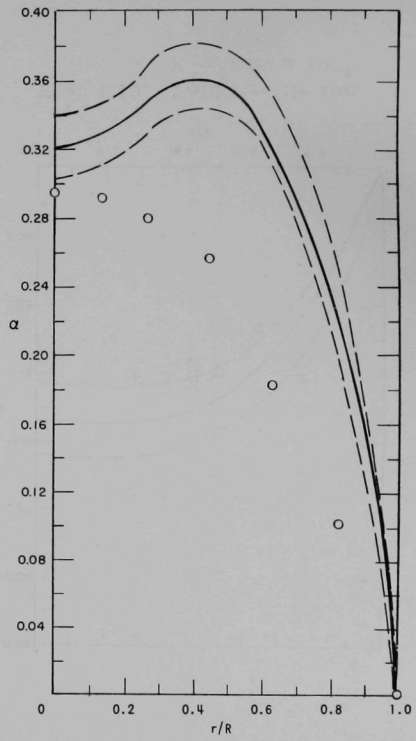

Fig. 4.7. Void Profile for $X = 10.45 \times 10^{-4}$

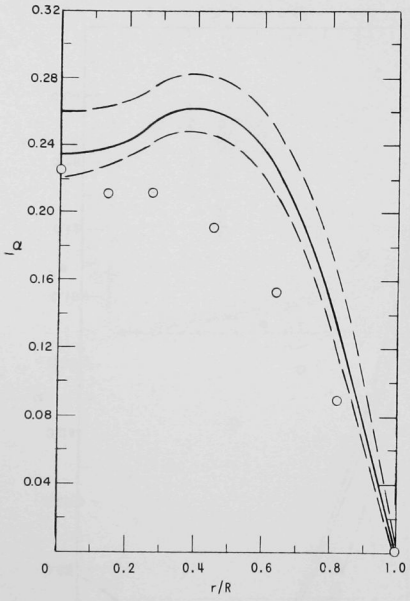

Fig. 4.8. Void Profile for $X = 6.82 \times 10^{-4}$

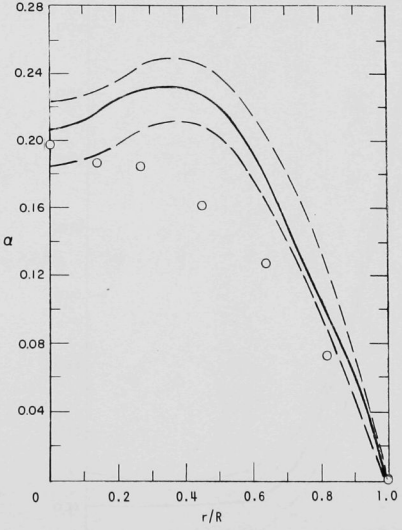

Fig. 4.9. Void Profile for $X = 4.48 \times 10^{-4}$

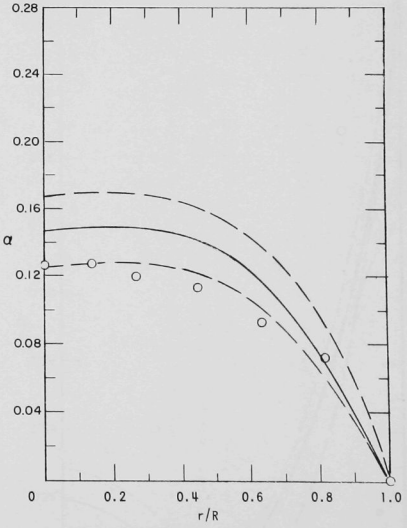

Fig. 4.10. Void Profile for $X = 3.09 \times 10^{-4}$

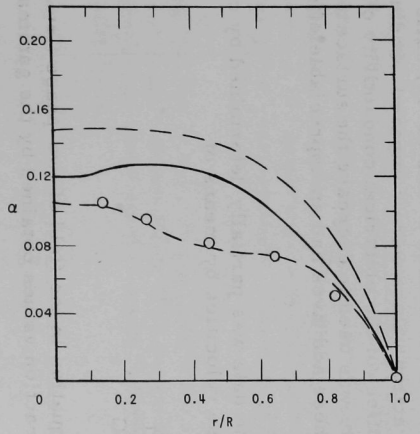

Fig. 4.11. Void Profile for $X = 2.24 \times 10^{-4}$

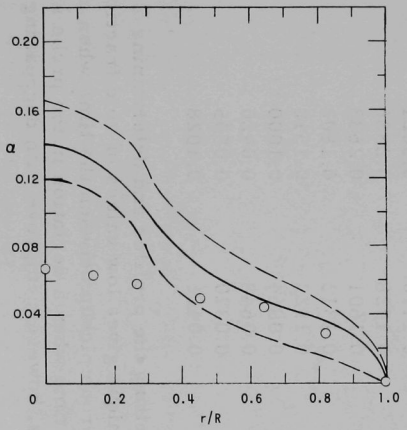

Fig. 4.12. Void Profile for $X = 1.25 \times 10^{-4}$

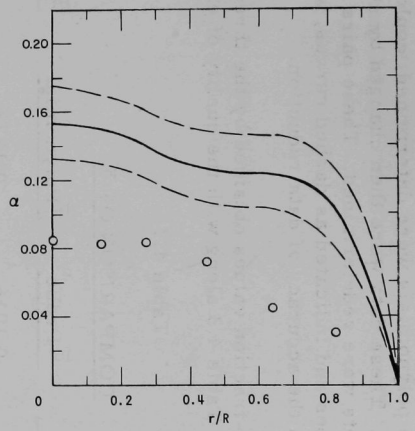

Fig. 4.13. Void Profile for $X = 1.60 \times 10^{-4}$

The data, from which the polynomials were determined, could be read to an accuracy of ±0.05 mv. These data were then changed by ±0.05 mv, and the polynomial coefficients were redetermined. These pairs of profiles, denoted as error envelopes and indicated as dashed curves, were plotted to show the sensitivity in the accuracy of data reduction.

The average void-fraction values obtained by the three different methods are tabulated in Table 4.3 along with the quality of each run.

Table 4.3

COMPARISON OF $\bar{\alpha}$

Run	Quality x 10^4	$\bar{\alpha}_{Probe}$	$\bar{\alpha}_{Polynomial}$	$\bar{\alpha}_{Traversed}$
1	5.35	0.1016	0.1878	0.1751
2	8.15	0.1710	0.3021	0.2867
3	6.48	0.1728	0.2326	0.2224
4	10.45	0.1601	0.2633	0.2451
5	6.82	0.1313	0.1802	0.1700
6	4.48	0.1123	0.1510	0.1498
7	3.09	0.0864	0.1000	0.1110
8	2.24	0.0648	0.0920	0.0838
9	1.25	0.0370	0.0505	0.0853
10	1.60	0.0466	0.1028	0.1106

The results of plotting the profiles and determining $\bar{\alpha}$ show that, in each run, the probe technique gives low values of void fraction. This could be due to a delay in the probe pickup between the time when the probe just pierces a bubble and the time when a deviation in the probe signal occurs. The probe technique does, however, improve with decreasing qualities.

In order to search for the source of this error, salts were dissolved in the water, and void-fraction values were compared. Sodium chloride was added to check the effect of the electrical conductivity of the water, and sodium ethyl xanthate was used to decrease the surface tension. As seen in Table 4.4 neither of these additives had an appreciable effect on the void measurements.

The validity of the data was partially determined by checking the ratio of the average phase velocities by means of

$$\frac{V_G}{V_L} = \frac{X}{1-X} \frac{1-\bar{\alpha}}{\bar{\alpha}} \frac{\rho_L}{\rho_G} \quad , \tag{4.8}$$

which is a well-known equation in the field of two-phase flow. The cross-sectional average void fraction values obtained by the gamma technique

were used in equation (4.8), resulting in velocity slip ratios in the range between 1.18 and 2.75. From previous experience, these are known to be reasonable.

Table 4.4

EFFECT OF ADDITIVES ON VOID FRACTION MEASUREMENTS

	Sodium Ethyl Xanthate	
α (no salt)	α (10 ppm added)	α (20 ppm added)
0.1082	0.1150	0.1062
0.1696	0.1832	0.1745
0.239	0.243	0.233

	Sodium Chloride
	α (190 ppm added)
0.1073	0.0926
0.1885	0.1496
0.239	0.215

The sensitivity of the electrical probe was determined by measuring the smallest pulse observed on the photographic record of the signals. The duration of the smallest pulse observed was $\frac{1}{64}$ in., which corresponds to a bubble dwell time of 0.0006 sec. If the bubble velocity is 2 ft/sec, this pulse resulted from a bubble having a diameter as small as 0.015 in. If, however, there is a delay in the system, as mentioned before, this pulse would be the result of a much larger bubble, and any bubble smaller than this one would not be detected at all.

One may have noticed that the polynomials approximating the void profiles were not always decreasing functions of the radius. This was probably due to the injection of air along the periphery of the test section such that the flow was not fully developed at the measuring point. To check this theory, a 100 mesh screen was inserted just above the mixer and the profiles were redetermined. The results are shown in Figures 4.14 and 4.15.

Although all the results do not favor the use of an electrical probe for local measurements of air-water flow parameters, further development of this probe may improve it to a point where it will become a very useful tool in this field.

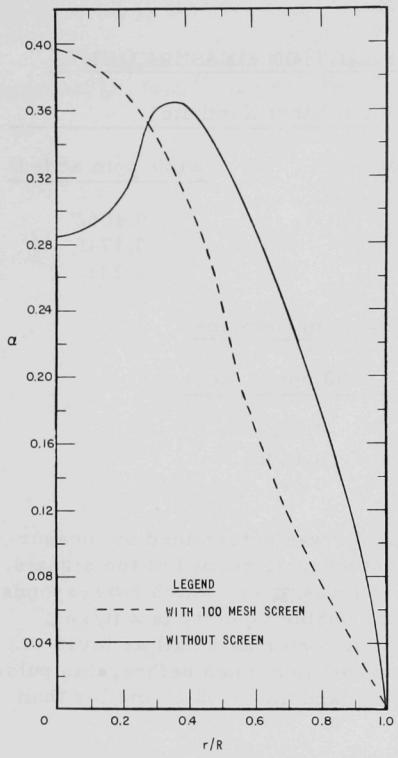

Fig. 4.14. Void Profile Dependence on Mixer; X = 6.38 x 10^{-4}

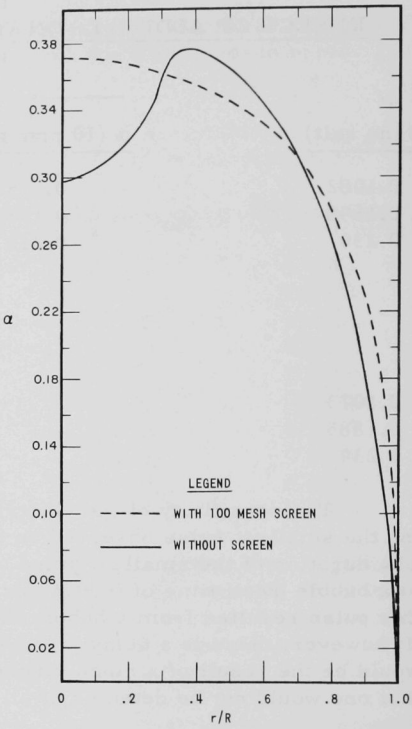

Fig. 4.15. Void Profile Dependence on Mixer; X = 10.45 x 10^{-4}

V. CONCLUSIONS

1. The electrical probe tip is wetted by the water and an irregularly shaped pulse results.

2. A triggering circuit incorporated in the integrating circuit employed improves the pulse shape, but the present technique still gives low values of local void fraction as compared with results from the gamma-ray technique.

3. The low electrical conductivity of water has little effect on measurements of void fraction.

4. Further development of this technique is necessary.

VI. APPENDIX

Table A-1

PROBE DATA

Run	r'	α	$\alpha_{corrected}$ (α_c)	$2\alpha_c r'$	Run	r'	α	$\alpha_{corrected}$ (α_c)	$2\alpha_c r'$
1	0.0	0.201		0.0	6	0.0	0.196	0.197	0.0
	0.136	0.198		0.055		0.136	0.186	0.187	0.052
	0.273	0.143		0.081		0.272	0.184	0.185	0.105
	0.454	0.133		0.121		0.454	0.160	0.161	0.146
	0.636	0.095		0.121		0.636	0.126	0.127	0.162
	0.818	0.082		0.135		0.818	0.080	0.080	0.132
	1.0	0.0		0.0		1.0	0.0	0.0	0.0
2	0.0	0.279		0.0	7	0.0	0.126	0.127	0.0
	0.136	0.263		0.72		0.136	0.127	0.128	0.036
	0.273	0.259		0.147		0.273	0.119	0.120	0.068
	0.454	0.233		0.213		0.454	0.112	0.113	0.103
	0.636	0.202		0.258		0.636	0.093	0.093	0.119
	0.818	0.133		0.218		0.818	0.073	0.073	0.120
	1.0	0.0		0.0		1.0	0.0	0.0	0.0
3	0.0	0.250	0.253	0.0	8	0.0	0.113	0.114	0.0
	0.136	0.245	0.248	0.68		0.136	0.104	0.105	0.029
	0.273	0.248	0.251	0.143		0.273	0.094	0.095	0.054
	0.454	0.214	0.217	0.198		0.454	0.081	0.082	0.075
	0.636	0.180	0.182	0.232		0.636	0.073	0.074	0.095
	0.818	0.088	0.089	0.146		0.818	0.050	0.050	0.082
	1.0	0.0	0.0	0.0		1.0	0.0	0.0	0.0
4	0.0	0.290	0.293	0.0	9	0.0	0.067	0.067	0.0
	0.136	0.286	0.289	0.079		0.136	0.063	0.063	0.018
	0.272	0.275	0.278	0.158		0.273	0.058	0.058	0.032
	0.454	0.253	0.256	0.233		0.454	0.050	0.050	0.046
	0.636	0.179	0.181	0.231		0.636	0.044	0.044	0.056
	0.818	0.099	0.100	0.163		0.818	0.029	0.029	0.048
	1.0	0.0	0.0	0.0		1.0	0.0	0.0	0.0
5	0.0	0.224	0.225	0.0	10	0.0	0.084	0.086	0.0
	0.136	0.210	0.211	0.058		0.136	0.082	0.084	0.023
	0.272	0.211	0.212	0.120		0.273	0.083	0.085	0.045
	0.454	0.190	0.191	0.174		0.454	0.071	0.073	0.065
	0.636	0.152	0.153	0.195		0.636	0.045	0.046	0.057
	0.818	0.089	0.089	0.146		0.818	0.030	0.031	0.049
	1.0	0.0	0.0	0.0		1.0	0.0	0.0	0.0

Table A-2

POLYNOMIAL COEFFICIENTS FOR PROFILES

Run	σ	a	b	c
1	0.2529	0.1172	-0.3887	0.0235
2	0.3495	0.5327	-1.7833	1.1227
3	0.3211	0.0430	-0.3258	-0.0055
4	0.3200	0.4647	-1.4921	0.8338
5	0.2341	0.3760	-1.2686	0.7009
6	0.2075	0.4043	-1.6811	1.2072
7	0.1478	0.0757	-0.5628	0.4081
8	0.0924	0.3363	-1.0626	0.6718
9	0.1417	-0.5347	0.9802	-0.6023
10	0.1539	-0.2485	0.6860	-0.6226

Table A-3

POLYNOMIAL COEFFICIENTS FOR UPPER ERROR ENVELOPE

Run	σ	a	b	c
1	0.2573	0.2328	-0.6888	0.2594
2	0.3667	0.4907	-1.6360	1.0186
3	0.3417	-0.0114	-0.0593	-0.2685
4	0.3380	0.4245	-1.2188	0.5404
5	0.2593	0.2766	-0.8937	0.3718
6	0.2231	0.4118	-1.6923	1.2326
7	0.1683	0.0165	-0.3450	0.2409
8	0.1477	0.0486	-0.4413	0.3017
9	0.1640	-0.5087	0.8119	-0.4162
10	0.1747	-0.2424	0.6637	-0.5872

Table A-4

POLYNOMIAL COEFFICIENTS FOR LOWER ERROR ENVELOPE

Run	σ	a	b	c
1	0.2224	0.5657	-2.1999	1.5888
2	0.3237	1.1535	-4.5138	3.5618
3	0.3054	0.0454	-0.3652	0.0272
4	0.3017	0.4996	-1.5751	0.8691
5	0.2223	0.3333	-1.1863	0.6394
6	0.1835	0.3976	-1.5317	1.0291
7	0.1249	0.0921	-0.5316	0.3380
8	0.1053	-0.2408	0.7048	-0.6948
9	0.1205	-0.5576	1.0596	-0.6853
10	0.1339	-0.2423	0.6915	-0.6676

VII. BIBLIOGRAPHY

1. Bankoff, S. G., A Variable Density Single Fluid Model for Two-phase Flow with Particular Reference to Steam-Water Flow, J. Heat Transfer, Trans. ASME, Series C, 82, 265 (1960).

2. Dengler, C. E., Heat Transfer and Pressure Drop for Evaporation of Water in a Vertical Tube, Ph.D. Thesis, MIT (1952).

3. Fluid Meters: Their Theory and Application, ASME Research Publication, 4th ed. (1937).

4. Gouse, S. W., Methods of Measuring Void Fractions, North American Aviation-SR-MEMO-5597 (1960).

5. Grace, H. P., and C. E. Lapple, Discharge Coefficients of Small-diameter Orifices and Flow Nozzles, Trans. ASME, 73, 639 (1951).

6. Hooker, H. H., and G. F. Popper, A Gamma-ray Attenuation Method for Void Fraction Determination in Steam-Water Mixtures, ANL-5766 (1958).

7. Johnson, H. A., and A. H. Abou-Sobe, Heat Transfer and Pressure Drop for Turbulent Flow of Air-Water Mixtures in a Horizontal Pipe, Trans. ASME, 74, 977 (1952).

8. Levy, S., Prediction of Two-phase Pressure Drop and Density Distribution from Mixing Length Theory, Trans. ASME, Paper No. 62-HT-6 (1962).

9. Neal, L. G., Local Parameters in Co-current Mercury-Nitrogen Flow, Ph.D. Thesis, Northwestern University (1962).

10. Petrick, M., A Study of Vapor Carryunder and Associated Problems, ANL-6581 (1962).

11. Petrick, M., Two-phase Air-Water Flow Phenomena, ANL-5787 (1958).

12. Solomon, J. V., Construction of a Two-phase Flow Regime Transition Detector, M.S. Thesis, MIT (1962).

13. Yusef, M., H. C. Perkins, Jr., and G. Leppert, A Void Measurement Technique for Local Boiling, Nuclear Science and Engineering, 1, 525 (1960).

14. Zuber, N., and J. Hench, Steady State and Transient Void Fraction of Bubbling Systems and Their Operating Limits, Part 1: Steady State Operation, General Engineering Laboratory Report No. 62GL 100 (1962).

VIII. ACKNOWLEDGEMENT

The author wishes to express his gratitude to Professor S. G. Bankoff of Northwestern University for his encouraging and helpful assistance during the course of this research.

This study was performed at Argonne National Laboratory under the AMU Program. The help of Dr. Michael Petrick and the people under his supervision is greatly appreciated. In particular, the author thanks Peter Zaleski who constructed the experimental apparatus, T. Theodore Anderson who designed part of the electronics system, and Carole Penosky who typed the original manuscript.

IX. NOMENCLATURE

C	electrical capacitance, farads
E	electrical voltage, v
$e(t)$	voltage signal from electrical probe, v
R	pipe radius, ft; electrical resistance, ohms
r	variable pipe radius, ft
r'	dimensionless variable radius, r/R
T	integration time, sec
t	variable time, sec
V_G	cross-sectional average gas velocity, ft/sec
V_L	cross-sectional average liquid velocity, ft/sec
W_G	gas mass flow rate, lb/sec
W_L	liquid mass flow rate, lb/sec
X	quality, dimensionless
α	local void fraction
α_r	radial distribution of void fraction
$\overline{\alpha}$	cross-sectional average void fraction
β	volumetric flow concentration
ρ_G	gas density, lb/ft^3
ρ_L	liquid density, lb/ft^3